DOI: 10.1002/ejic.201100043

Structural Effects of Varied Steric Bulk in 2,(4),6-Substituted Dimethylthallium(III) Phenoxides

Glen G. Briand,*[a] Andreas Decken,[b] J. Ian McKelvey,[a] and Yukun Zhou[a]

Keywords: Thallium / O ligands / Density functional calculations / Structure elucidation

The structural effects of varied steric bulk on 2,(4),6-substituted dimethylthallium(III) phenoxides has been examined. The facile reaction of Me_3Tl with a series of 2,(4),6-substituted phenols in toluene or diethyl ether resulted in the formation of the species $[Me_2TlO(2,6\text{-}R_2C_6H_3)]_2$ [R = H (**4**), Me (**5**), *i*Pr (**6**), Ph (**7**)] and $[Me_2TlO(2,4,6\text{-}t\text{Bu}_3C_6H_2)]$ (**8**). All compounds have been characterized by elemental analysis as well as their melting point; FTIR, FT-Raman, solution ^1H and $^{13}C\{^1H\}$ NMR spectroscopy; and X-ray crystallography. The structures of **4**–**7** are dimeric through short intermolecular Tl–O interactions, which yield a symmetric Tl_2O_2 unit and a distorted seesaw C_2O_2 bonding environment for thallium. An increase in the steric bulk in **4**–**6** has little effect on Tl–O bond lengths, whereas the C_{Me}–Tl–C_{Me} bond angle was found to significantly decrease. Further, the phenoxide ligands in **5** and **6** were found to be oriented perpendicular to the Tl_2O_2 unit to minimize steric interactions. Alternatively, compound **7** shows an increase in Tl–O bond lengths and an increase in the C_{Me}–Tl–C_{Me} bond angle compared to **4**–**6**, and orientation of the phenoxide ligands perpendicular to the Tl_2O_2 core. The significant steric bulk imposed by the –$O(2,4,6\text{-}t\text{Bu}_3C_6H_2)$ ligand in **8** precludes dimer formation and allows for isolation of a monomeric species that contains a three-coordinate T-shaped C_2O bonding environment for thallium. DFT calculations show that the energetic favorability of dimer formation decreases with increased phenoxide steric bulk.

Introduction

Although the facile preparation of thin films of thallium-based high-T_c superconductors (TlBaCaCuO)[1] and semiconductors (Tl_2O_3)[2] by means of metal–organic chemical-vapor deposition (MOCVD) was first demonstrated some time ago,[3,4] there have been very few studies of potential organometallic thallium oxide precursors.[5,6] Potential "single source" candidates include diorganothallium(III) compounds (e.g., R_2TlOR'), which comprise the most stable and extensively studied class of organothallium(III) species.[7] However, intermolecular Tl···O interactions in these compounds result in dimeric or polymeric species in the solid state {e.g., $[Ph_2Tl(trop)]_2$ (**1**; trop = tropolonate), $[Me_2Tl(acac)]_\infty$ (**2**; acac = acetylacetonate)}[8–10] and likely decrease their volatility.

Simple dimethylthallium alkyl/aryloxide species have been known for some time, though few examples have been reported in the literature, namely, Me_2TlOR [R = Me,[11] Et,[12] *t*Bu,[13] 2-ClC_6H_4 (**3**),[14] 2-$(CHO)C_6H_4$,[15] C_6H_5 (**4**)].[15,16] Further, many of these compounds are poorly characterized and/or detailed synthetic procedures are not provided. Structural characterization of **3** and **4** has shown that these species are dimeric in the solid state through very short intermolecular Tl–O bonding interactions, which yield a strongly bonded and symmetric Tl_2O_2 unit.[14] These complexes also feature near-linear C_{Me}–Tl–C_{Me} bond angles and a peculiar distorted seesaw geometry at thallium, which valence-shell electron-pair repulsion (VSEPR) theory predicts to be tetrahedral given the absence of a valence lone pair of electrons at the metal center. To determine the effect of altering the steric bulk on the formation of intermolecular bonds and the bonding environment of thallium in dimethylthallium phenoxide species,[17] we have prepared and structurally characterized the complexes $[Me_2TlO(2,6\text{-}R_2C_6H_3)]_2$ [R = H (**4**), Me (**5**), *i*Pr (**6**), Ph (**7**)] and $[Me_2TlO(2,4,6\text{-}t\text{Bu}_3C_6H_2)]$ (**8**), which incorporate bulky 2,(4),6-substituted phenoxide ligands. Further, we have studied the subtle changes in the resulting thallium bonding environments by means of vibrational and solution NMR spectroscopy, and carried out DFT calculations to rationalize the observed structures.

[a] Department of Chemistry and Biochemistry, Mount Allison University,
Sackville, New Brunswick, E4L 1G8, Canada
Fax: +1-506-364-2313
E-mail: gbriand@mta.ca
[b] Department of Chemistry, University of New Brunswick, Fredericton, New Brunswick, E3B 6E2, Canada

Supporting information for this article is available on the WWW under http://dx.doi.org/10.1002/ejic.201100043.

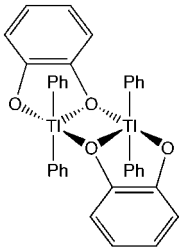

1

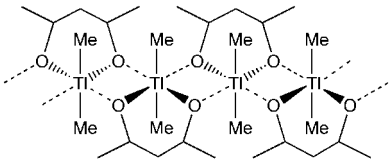

2

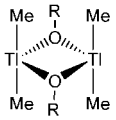

R = C_6H_5 (**4**)
2,6-$Me_2C_6H_3$ (**5**)
2,6-$iPr_2C_6H_3$ (**6**)
2,6-PhC_6H_3 (**7**)

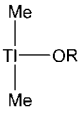

R = 2,4,6-$tBu_3C_6H_2$ (**8**)

Results and Discussion

Syntheses

The hydrocarbon elimination reaction between trimethylthallium and the corresponding alcohol[13] is desirable due to the high reactivity of the triorganothallium species to rapidly yield the more stable diorganothallium alkoxide and methane reaction byproduct. Trimethylthallium is prepared in moderate yield by means of a redox reaction between thallium(I) iodide, methyl iodide, and methyllithium in diethyl ether, and may be isolated by means of fractional sublimation of the volatile product from the crude reaction product at –26 °C.[18]

The reaction of Me_3Tl with HOPh in diethyl ether to yield **4** occurred rapidly at room temperature with evolution of methane gas, whereas the rate of reaction appeared to decrease as the 2,6-disubstituted phenol steric bulk was increased to yield **5**–**8**. All reactions were complete within one hour, and the products were isolated by slow evaporation or cooling of reaction mixtures. All reactions were quantitative, as determined from ^1H NMR spectra of the reaction mixtures. The reported yields (13–48%) are of crystalline material obtained from the reaction filtrate.

Solution NMR Spectroscopy Studies

Solution ^1H NMR studies of **4**–**8** in [D_6]DMSO showed a narrow range of $^2J(^1H–^{203/205}Tl)$ values (420–431 Hz), whereas the Me_2Tl resonance of **7** (δ = 0.47 ppm) was upfield from those of **4**–**6** and **8** (δ = 0.71–0.85 ppm).[19] The corresponding $^{13}C\{^1H\}$ NMR spectra show a narrow range of Me_2Tl– resonances for **4**–**7** (δ = 23.0–24.4 ppm), whereas the $^1J(^{13}C–^{203/205}Tl)$ value is significantly smaller for **7** (**4**–**6**: 2922–2963 Hz; **7**: 2811 Hz). The $^{13}C\{^1H\}$ NMR resonance for **8** (δ = 26.6 ppm) is slightly downfield from that of **4**–**7**, whereas the corresponding $^1J(^{13}C–^{203/205}Tl)$ value (2882 Hz) is in a similar range. Overall, chemical-shift values and coupling constants do not appear to correspond to changes in the $C_{Me}–Tl–C_{Me}$ bond angle or Tl–O bond lengths observed in the solid-state structures (vide infra).

Vibrational Spectroscopy

The vibrational spectra of **4**–**8** all show characteristic peaks that correspond to the symmetric and asymmetric stretching vibrations of the Me–Tl–Me unit. Due to the near-linear and centrosymmetric nature of the dimethylthallium groups in **4**–**7**, the symmetric vibration is very strong in the FT-Raman spectra and very weak in the corresponding FTIR spectra, whereas the opposite is observed for the asymmetric mode. The frequencies for each molecular vibration in **4**–**8** fall in a relatively narrow range [ν_{sym}(Me–Tl–Me) = 473–484 cm^{-1}; ν_{asym}(Me–Tl–Me) = 527–546 cm^{-1}] and are typical for dimethylthallium species.[15,16,20] As in the case of the solution NMR spectroscopic resonances, the ν_{sym}(Me–Tl–Me) and ν_{asym}(Me–Tl–Me) do not correspond to the changes in the $C_{Me}–Tl–C_{Me}$ bond angle or Tl–O bond lengths observed in the solid-state structures.

Crystal Structure Determination

Crystals suitable for X-ray crystallographic analysis were isolated for **4**–**8** by the slow evaporation of reaction mixtures at 23 °C. Selected bond lengths and angles are given in Table 1. The structure of **5** contains two independent molecules in the asymmetric unit. Although the structure of **4** has been reported previously,[21] structural parameters are not available on the CCDC and we have redetermined the structure for comparisons with **5**–**8**.

The structures of $[Me_2TlO(2,6\text{-}R_2C_6H_3)]_2$ [R = H (**4**), Me (**5**), *i*Pr (**6**), Ph (**7**)] (Figures 1, 2, 3, and 4) show dimerization of the corresponding dimethylthallium phenoxide through intermolecular Tl···O contacts. The Tl–O bond lengths of the resulting near-planar Tl_2O_2 cores are similar, and no monomeric unit can be identified. This is in contrast to the thiolate analogue of **4**, namely, $[Me_2TlS(C_6H_5)]_2$, in which the Tl–S bond lengths differ by 0.243(8) Å (9%).[14] The result is a four-coordinate C_2O_2 bonding environment for Tl. Given the lack of a valence lone pair for thallium(III), a tetrahedral geometry is expected at the metal center. However, the $C_{Me}–Tl–C_{Me}$ bond angles [167.8(8) and 166.9(8)°] are significantly larger than the ideal 109.5° in **4**, whereas the O–Tl–O bond angles [75.2(4)–75.5(4)°] were found to be significantly smaller. The latter is likely a result of the constraints imposed by the formation of a four-membered Tl_2O_2 ring. The distortion from an ideal tetrahedron is quite significant, and is best described as a distorted seesaw geometry at Tl (vide infra).

2,6-Disubstitution of the phenoxide ligands in **5** and **6** yields some distortions in the molecular framework compared to the unsubstituted analogue **4**. Firstly, all four methyl groups in **4** are in the same plane, and the two $C_{Me}–$

Table 1. Selected bond lengths [Å] and angles [°] for **4**–**8**.

	4	**5**	**6**	**7**	**8**
Tl1–C1	2.15(2)		2.132(3)	2.131(5)	2.112(5)
Tl1–C2	2.13(2)		2.141(4)	2.130(5)	2.123(5)
Tl1–C9		2.123(1)			
Tl1–C10		2.12(1)			
Tl1–O1	2.39(1)	2.417(6)	2.415(2)	2.521(3)	2.283(3)
Tl1–O2	2.38(1)	2.412(6)		2.505(3)	
Tl1–O1*			2.397(2)		
Tl2–C3	2.16(2)			2.126(5)	
Tl2–C4	2.12(2)			2.130(5)	
Tl2–C19		2.13(1)			
Tl2–C20		2.14(1)			
Tl2–O1	2.38(1)	2.386(6)		2.532(3)	
Tl2–O2	2.38(1)	2.370(6)		2.484(3)	
Tl3–C29		2.12(1)			
Tl3–C30		2.14(1)			
Tl3–O3		2.388(6)			
Tl3–O4		2.393(7)			
Tl4–C39		2.14(1)			
Tl4–C40		2.14(1)			
Tl4–O3		2.407(7)			
Tl4–O4		2.399(6)			
C1–Tl1–C2	167.8(8)		156.9(2)	169.1(2)	170.2(2)
C3–Tl2–C4	166.9(8)			171.9(2)	
C9–Tl1–C10		160.4(4)			
C19–Tl2–C20		158.7(4)			
C29–Tl3–C30		157.1(4)			
C39–Tl4–C40		158.0(4)			
O1–Tl1–O2	75.2(4)	73.3(2)		88.1(1)	
O1–Tl2–O2	75.5(4)	74.6(2)		88.4(1)	
O3–Tl3–O4		74.0(2)			
O3–Tl4–O4		73.6(2)			
O1–Tl1–O1*			76.22(7)		
C1–Tl1–O1					88.0(2)
C2–Tl1–O1					101.8(2)

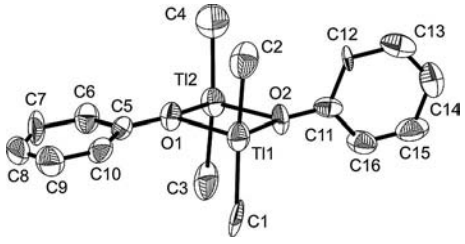

Figure 1. Crystal structure of **4** (50% probability ellipsoids). Hydrogen atoms are not shown for clarity.

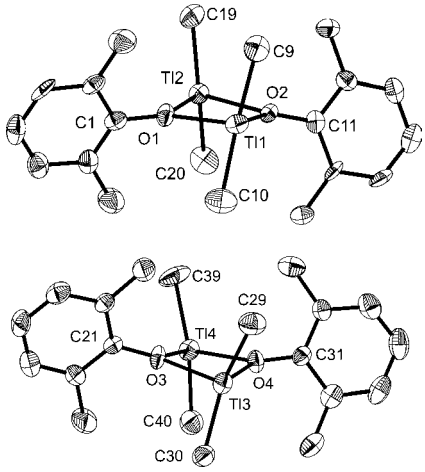

Figure 2. Crystal structure of the two crystallographically unique molecules of **5** (50% probability ellipsoids). Hydrogen atoms are not shown for clarity.

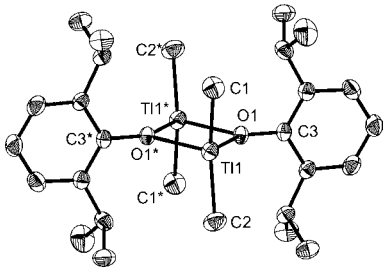

Figure 3. Crystal structure of **6** (50% probability ellipsoids). Hydrogen atoms are not shown for clarity. Symmetry transformations used to generate equivalent atoms: (*) $-x + 1, -y + 1, -z + 2$.

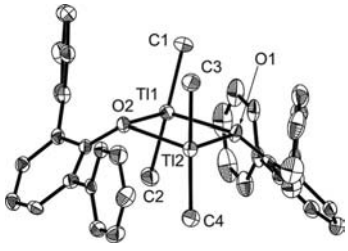

Figure 4. Crystal structure of **7** (50% probability ellipsoids). Hydrogen atoms are not shown for clarity.

Tl–C_{Me} units form 88.4(4)° and 88.7(5)° angles with the Tl_2O_2 ring. One phenyl ring (C5–C10) is nearly coplanar with the Tl_2O_2 core [16.4(8)°], whereas the second (C11–C15) is nearly orthogonal [84.7(4)°]. In **5** and **6**, the 2,6-disubstituted phenoxide ligands are nearly coplanar with one another and orthogonal to the distorted Tl_2O_2 core. Although this presumably occurs to minimize steric crowding of the C_{Me}–Tl–C_{Me} unit, a decrease of the C_{Me}–Tl–C_{Me} bond angle by approximately 10° is observed. Further, the two C_{Me}–Tl–C_{Me} units in each structure are rotated with respect to one another and are oriented 78.5(7)–83.1(4)° (**5**) and 85.8(1)° (**6**) to the Tl_2O_2 ring. However, there are no significant changes in the Tl–C or Tl–O bond lengths or the O–Tl–O bond angles. The similar structural effects imposed by both the 2,6-dimethyl and 2,6-diisopropyl substitution is not surprising, given the orientation of the isopropyl groups away from the center of the molecule in **6** (Figure 3). This results in similar degrees of steric crowding at the thallium-bonded methyl groups in **5** and **6**. The overall structural arrangement of **5** is similar to that of the indium analogue $[Me_2InO(2,6\text{-}Me_2C_6H_3)]_2$,[22] whereas **6** resembles the aluminum analogue $[Me_2AlO(2,6\text{-}i Pr_2C_6H_3)]_2$.[23]

Contrary to the decrease in the C_{Me}–Tl–C_{Me} bond angle observed in **5** and **6**, that of the 2,6-diphenylphenoxide analogue **7** [C1–Tl1–C2 169.1(2)° and C3–Tl1–C4 171.9(2)°] was found to be greater than in **4**–**6** [156.9(2)° and

167.8(8)°]. The O–Tl–O bond angles [88.1(1) and 88.4(1)°] are also significantly greater than in **4**–**6** [73.3(2)–75.5(4)°]. Although the Tl–C_{Me} bond lengths in **7** are similar to those in **4**–**6**, the Tl–O bond lengths are significantly longer [**7**: 2.484(3)–2.532(3) Å; **4**–**6**: 2.38(1)–2.417(6) Å]. As with **5** and **6**, the C_{Me}–Tl–C_{Me} units are rotated with respect to one another [15.0(9)°] and are oriented at 85.0(6)° and 85.5(4)° to the near-planar Tl_2O_2 core. Perhaps the most significant structural change is a decrease in the sum of the bond angles at O, thereby resulting in *cis*-type orientation of the phenoxide rings relative to the Tl_2O_2 ring, and angles of 42.4(1)° and 51.7(1)° between the phenoxide rings and the Tl_2O_2 plane. Further, unlike **5** and **6**, the phenoxide groups of **7** are not oriented orthogonal to the Tl_2O_2 core. Finally, the 2,6-diphenyl substituents are rotated with respect to the central phenoxide rings, presumably to allow for minimum steric repulsion with the $(Me_2TlO)_2$ core, as well as between 2,6-$Ph_2C_6H_3O$ groups. The structure of **7** differs from that of the aluminum analogue [Me_2AlO(2,6-$Ph_2C_6H_3$)]$_2$, which has a structural arrangement similar to **5** and **6**.[24]

In contrast to **4**–**7**, the structure of [Me_2TlO(2,4,6-tBu$_3C_6H_2$)] (**8**) (Figure 5) shows the compound to be monomeric in the solid state. The Tl–C_{Me} bond lengths [2.112(5) and 2.123(5) Å] are slightly shorter than those observed for **4**–**7**, while the Tl–O bond length [2.283(3) Å] is significantly shortened. The nearest intermolecular Tl···O contact is 3.612(3) Å, and is outside of the sum of the van der Waals radii of 3.5 Å.[25] The bond angles at thallium [C1–Tl1–C2 170.2(2)°; C1–Tl1–O1 88.0(2)°; C2–Tl1–O1 101.8(2)°] are significantly different from 120°, as predicted by valence-shell electron-pair repulsion (VSEPR) theory, and the geometry is best described as distorted T-shaped. The Me–Tl–Me unit is aligned orthogonal to the phenoxy ring, which minimizes steric repulsion with the *t*Bu substituents. The monomeric structure is similar to that observed for the indium analogue [Me_2InO(2,4,6-tBu$_3C_6H_2$)].[22]

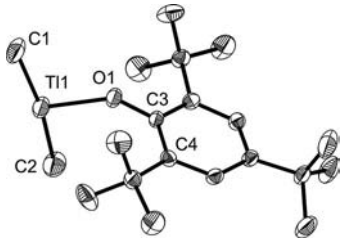

Figure 5. Crystal structure of **8** (50% probability ellipsoids). Hydrogen atoms are not shown for clarity.

DFT Computational Studies

DFT calculations were performed to provide insight into the observed solid-state structures. Structural representations of the geometry-optimized structures are shown in Figure 6. Energies for geometry-optimized structures are given in Table 2.

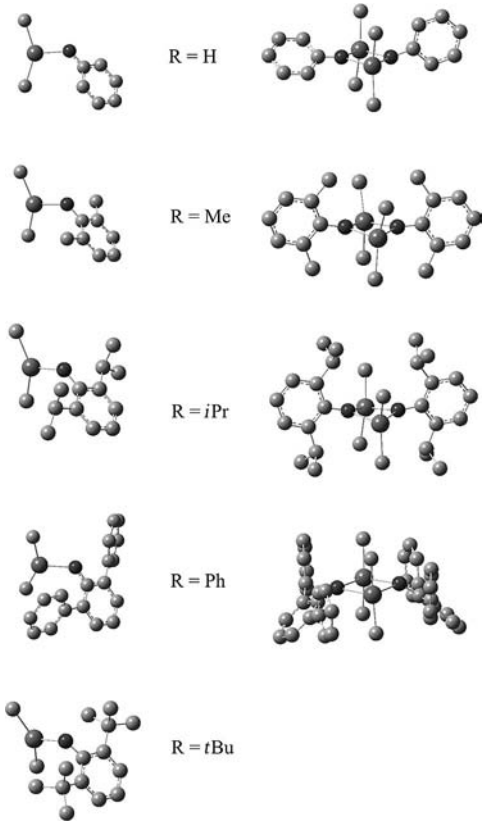

Figure 6. Geometry-optimized structures of monomeric and dimeric Me_2TlO(2,6-$R_2C_6H_3$) species. Hydrogen atoms are not shown for clarity.

In the calculated R = Me, *i*Pr, and *t*Bu monomers, the phenoxide rings are near orthogonal to the Me_2Tl unit, as observed in the solid-state structure of **8**. This presumably minimizes steric repulsion among the Me_2Tl methyl groups and the phenoxide 2,6-substituents. Alternatively, the R = H monomer, which is not sterically impeded, shows an angle of around 54° between the phenoxide ring and the Me_2Tl unit. The phenoxy ring in the R = Ph monomer shows a "twisted" orientation versus the Me_2Tl unit [∠ C_{Me}–Tl–O–C_{ipso} 24°; ∠ Tl–O–C_{ipso}–C_{ortho} 53°], similar to the arrangement observed in the solid-state structure of

Table 2. Calculated energies (E) [kJ mol^{-1}] for geometry optimized monomeric (m) and dimeric (d) Me_2TlO(2,6-$R_2C_6H_3$) species.

	E				
	R = H	R = Me	R = *i*Pr	R = Ph	R = *t*Bu
Me_2Tl–O(2,6-$R_2C_6H_3$) (m)	–1,019,940	–1,226,248	–1,638,799	–2,232,777	–1,845,034
[Me_2Tl–O(2,6-$R_2C_6H_3$)]$_2$ (d)	–2,040,019	–2,452,607	–3,277,699	–4,465,601	–
$E_{dimerization}$ (d – 2m)	–139	–111	–101	–47	–

7. This suggests that the unique structure of **7** may be the result of a weak association of monomeric [$Me_2TlO(2,6\text{-}Ph_2C_6H_3)$] units. The overall structural arrangements of the R = H, Me, *i*Pr, and Ph dimers are similar to those obtained from the X-ray crystallographic data for **4**–**7**. It is also worth noting that the phenyl rings in the R = H dimer are rotated by approximately 55° with respect to the one another, closely resembling the orientation found in the solid-state structure of **4**.

To rationalize the observed intermolecular Tl–O bonding in **4**–**7**, the relative stabilities of the corresponding monomeric versus dimeric species may be calculated according to Equation (1).

$$2Me_2Tl\text{–}O(2,6\text{-}R_2C_6H_3) \rightarrow [Me_2Tl\text{–}O(2,6\text{-}R_2C_6H_3)]_2 \quad (1)$$

Negative values were obtained for Equation (1) (Table 2) for R = H, Me, *i*Pr, and Ph, thus indicating that dimer formation is thermodynamically favorable in each case. However, the energy lost through dimerization decreases significantly with increased steric bulk of the disubstituted phenoxide: R = H > Me > *i*Pr > Ph. In the case of R = *t*Bu, the dimeric structure geometry optimized to two monomeric compounds, thereby suggesting that the increase in energy from the steric strain imposed by the larger *t*Bu groups outweighs the energy decrease afforded by dimerization, that is, the formation of two intermolecular Tl···O bonds. This again is in agreement with the X-ray crystallographic analyses.

Although discrepancies are to be expected between calculated gas-phase structures and solid-state crystal structures, the results of DFT calculations were further analyzed in attempt to rationalize the near-linear [156.9(2)–171.9(2)°] C_{Me}–Tl–C_{Me} bond angles in the solid-state structures of dimeric compounds **4**–**7**. The C_{Me}–Tl–C_{Me} bond angles in the geometry-optimized structures are around 10–20° less than those in the corresponding crystal structures (see the Supporting Information). The calculated bending mode [δ(Me–Tl–Me) ≈ 150 cm^{-1}] is of very low frequency, thereby suggesting that the C_{Me}–Tl–C_{Me} bond angle may be easily perturbed by packing forces. Nevertheless, the overall symmetry of the dimeric structures is retained, and the calculated orbitals should be largely unaffected by small changes in the C_{Me}–Tl–C_{Me} bond angle. It should be noted that [$Me_2AlO(2,6\text{-}R_2C_6H_3)]_2$ [R = *i*Pr, Ph] have C_{Me}–Al–C_{Me} bond angles in the 114.3(6)–116.9(2)° range, whereas [$Me_2InO(2,6\text{-}Me_2C_6H_3)]_2$ has a C_{Me}–In–C_{Me} bond angle of 131.0(2)°.[22–24] Therefore, the (acute) calculated C_{Me}–Tl–C_{Me} angles are still significantly greater than those observed for structurally characterized aluminum and indium analogues. The difference is even more significant in the monomeric structures, in which the C_{Me}–In–C_{Me} bond angle of [$Me_2InO(2,4,6\text{-}tBu_3C_6H_2)$] is 109.3(8)° and the C_{Me}–Tl–C_{Me} bond angle of **8** is 170.2(2)°.

Analysis of the HOMO to HOMO–15 surfaces of [$Me_2TlO(2,6\text{-}Me_2C_6H_3)]_2$ (**5**) (Figure 7; see Supporting Information) shows that the majority are σ and π orbitals of the ($2,6\text{-}Me_2C_6H_3O$) ligands. Alternatively, HOMO–6 is a Tl(6p)–C(2p) σ-bonding orbital of the Me_2Tl groups. Of the molecular orbitals that involve Tl–O orbital overlap, HOMO–7 and HOMO–4 exhibit corresponding Tl(6p)–O(2p) π-bonding and π-antibonding interactions, respectively, whereas HOMO–8, –11, –14, and –15 exhibit Tl(6s)–O(2p) σ-antibonding orbital overlap. Further, analyses of atomic charges shows an overall +0.543 charge for the Me_2Tl groups and a corresponding –0.543 charge for the ($2,6\text{-}Me_2C_6H_3O$) ligands. These findings suggest that there is little net orbital bonding character between the ($2,6\text{-}Me_2C_6H_3O$) ligands and Me_2Tl groups, and the Tl–O bonding interaction appears to be largely electrostatic in nature. Therefore, the Me_2Tl groups are effectively isoelectronic with Me_2Tl^+ group, which is predicted to adopt a linear geometry according to VSEPR theory.

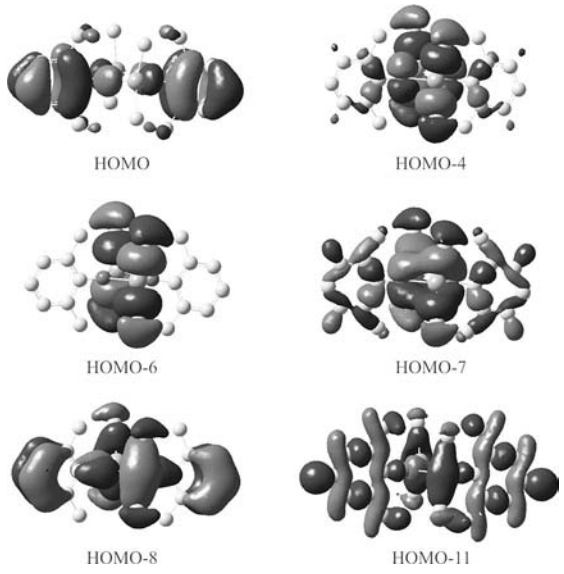

Figure 7. Selected DFT-calculated molecular orbitals of [$Me_2TlO(2,6\text{-}Me_2C_6H_3)]_2$ (**5**).

Conclusion

The effect of increasing steric bulk on the dimerization of dimethylthallium(III) phenoxides has been examined. The structures of **4**–**7** are dimeric through short intermolecular Tl–O interactions, which yield symmetric Tl_2O_2 cores. Increasing steric bulk in **4**–**6** has little effect on Tl–O bond lengths, whereas compound **7** shows an increase in Tl–O bond lengths, as well as a variety of other structural distortions to minimize steric crowding. The excessive steric bulk imposed by the *t*Bu substituents in **8** allows the preclusion of intermolecular Tl···O contacts and the isolation of a unique example of a monomeric species. Solution NMR and solid-state vibrational spectra show characteristic resonances for the dimethylthallium group, and are not useful for probing subtle structural changes or differentiating monomer versus dimer formation. DFT calculations of **4**–**7** and their dimeric/monomeric counterparts show that thermodynamic instability imposed by a moderately sterically bulky phenoxide ligand is more than compensated for by the formation of the intermolecular Tl···O bonds. How-

ever, the structural constraints imposed by the introduction of significant steric bulk (**8**) is sufficient to destabilize these bonding interactions and yield a monomeric dimethylthallium phenoxide species. It is thus clear from this study that intermolecular thallium–oxygen bonding interactions are very favorable, and are not effectively precluded with the introduction of a modest amount of steric bulk. To further explore intermolecular thallium–chalcogen bonding interactions in this class of compound, we are currently examining analogous dimethylthallium thiolate, selenolate, and tellurolate species.

Experimental Section

General Considerations: 2,6-Dimethylphenol (99%), 2,6-diisopropylphenol (97%), 2,6-di-*tert*-butylphenol (98%), 2,6-diphenylphenol (98%), 2,4,6-tri-*tert*-butylphenol (99%), methyllithium 1.6 M in diethyl ether, thallium(I) iodide (99.999%), and iodomethane (99.5%) were purchased from the Aldrich Chemical Co. 2,6-Diisopropylphenol (97%) was redistilled from CaO prior to use. Me_3Tl was prepared as reported previously and isolated by fractional sublimation at –26 °C.[18] All reactions were carried out under dinitrogen atmosphere using standard Schlenk techniques.

Caution: Thallium is a cumulative poison that may be absorbed through the skin. All compounds must be handled with extreme care.

Solution ^1H and $^{13}C\{^1H\}$ NMR spectra were recorded at 23 °C with a JEOL GMX 270 MHz spectrometer (270.2 and 67.9 MHz, respectively) or a Varian MERCURYplus 200 MHz spectrometer (200.0 and 50.3 MHz, respectively), and chemical shifts are calibrated to the residual solvent signal. FTIR spectra were recorded as Nujol mulls with KBr plates with a Mattson Genesis II FTIR spectrometer in the range of 4000–400 cm^{-1}. FT-Raman spectra were recorded with a Thermo Nicolet NXR 9600 Series FT-Raman spectrometer in the range of 3900–70 cm^{-1}. Melting points were recorded with an Electrothermal MEL-TEMP melting point apparatus and are uncorrected. Elemental analyses were performed by Chemisar Laboratories Inc., Guelph, Ontario.

$[Me_2TlO(C_6H_5)]_2$ (4): C_6H_5OH (0.095 g, 1.0 mmol) was added to a solution of $TlMe_3$ (0.250 g, 1.0 mmol) in toluene (5 mL). The solution was stirred for 1 h, filtered, and concentrated to 3 mL. The solution was allowed to sit at 23 °C for 3 d and filtered to yield **4** as colorless crystals (0.108 g, 0.33 mmol, 33%). $C_{16}H_{22}O_2Tl_2$ (655.08): calcd. C 29.33, H 3.39, N 0.00; found C 29.61, H 3.53, N < 0.10; m.p. 212–213 °C. FTIR: $\tilde{\nu}$ = 479 [w, ν_{sym}(Me–Tl–Me)] , 541 [s, ν_{asym}(Me–Tl–Me)]. FT-Raman: 480 [vs, ν_{sym}(Me–Tl–Me)], 538 [vw, ν_{asym}(Me–Tl–Me)] cm^{-1}. ^1H NMR ([D$_6$]DMSO): δ = 0.84 [d, $^2J_{Tl,H}$ = 426 Hz, 12 H, $Me_2TlO(C_6H_5)$], 6.24 [t, $^3J_{H,H}$ = 7.0 Hz, 2 H, $Me_2TlO(C_6H_5)$], 6.39 [d, $^3J_{H,H}$ = 7.4 Hz, 4 H, $Me_2TlO(C_6H_5)$], 6.90 [m, 4 H, $Me_2TlO(C_6H_5)$] ppm. $^{13}C\{^1H\}$ NMR ([D$_6$]DMSO): δ = 23.4 [d, $^1J_{Tl,^{13}C}$ = 2963 Hz, $Me_2TlO(C_6H_5)$], 112.9 [s, $Me_2TlO(C_6H_5)$], 119.4 [s, $Me_2TlO(C_6H_5)$], 129.2 [s, $Me_2TlO(C_6H_5)$], 167.9 [s, $Me_2TlO(C_6H_5)$] ppm.

$[Me_2TlO(2,6\text{-}Me_2C_6H_3)]_2$ (5): 2,6-$Me_2C_6H_3OH$ (0.120 g, 1.00 mmol) was added to a solution of $TlMe_3$ (0.250 g, 1.00 mmol) in toluene (5 mL). The solution was stirred for 1 h and filtered. The resulting colorless product was then dissolved in THF (1 mL), layered with diethyl ether (3 mL), and was allowed to sit at 23 °C. After 2 d, the solution was filtered to yield **5** as colorless crystals (0.085 g, 0.24 mmol, 24%). $C_{20}H_{30}O_2Tl_2$ (711.18): calcd. C 33.78, H 4.25, N 0.00; found C 34.13, H 4.26, N < 0.10; m.p. 166 °C. FTIR: $\tilde{\nu}$ = 528 [w, ν_{asym}(Me–Tl–Me)]. FT-Raman: 473 [vs, ν_{sym}(Me–Tl–Me)], 527 [vw, ν_{asym}(Me–Tl–Me)]. ^1H NMR ([D$_6$]-DMSO) δ = 0.73 [d, $^2J_{Tl,H}$ = 421 Hz, 12 H, $Me_2TlO(2,6\text{-}Me_2C_6H_3)$], 2.05 [s, 12 H, $Me_2TlO(2,6\text{-}Me_2C_6H_3)$], 6.02 [t, $^3J_{H,H}$ = 7.2 Hz, 2 H, $Me_2TlO(2,6\text{-}Me_2C_6H_3)$], 6.69 [d, $^3J_{H,H}$ = 7.2 Hz, 4 H, $Me_2TlO(2,6\text{-}Me_2C_6H_3)$] ppm. $^{13}C\{^1H\}$ NMR ([D$_6$]DMSO): δ = 18.8 [s, $Me_2TlO(2,6\text{-}Me_2C_6H_3)$], 23.2 [d, $^1J_{Tl,^{13}C}$ = 2926 Hz, $Me_2TlO(2,6\text{-}Me_2C_6H_3)$], 111.2 [s, $Me_2TlO(2,6\text{-}Me_2C_6H_3)$], 126.4 [s, $Me_2TlO(2,6\text{-}Me_2C_6H_3)$], 127.5 [s, $Me_2TlO(2,6\text{-}Me_2C_6H_3)$], 166.4 [s, $Me_2TlO(2,6\text{-}Me_2C_6H_3)$] ppm.

$[Me_2TlO(2,6\text{-}iPr_2C_6H_3)]_2$ (6): 2,6-$iPr_2C_6H_3OH$ (0.178 g, 1.00 mmol) was added to a solution of $TlMe_3$ (0.250 g, 1.00 mmol) in toluene (10 mL). After stirring for 1 h, the clear solution was concentrated to 5 mL, layered with hexane (1 mL), and allowed to sit at –15 °C. After 7 d, the solution was filtered to yield **6** as colorless crystals (0.196 g, 0.48 mmol, 48%). $C_{28}H_{46}O_2Tl_2$ (823.39): calcd. C 40.84, H 5.63, N 0.00; found C 41.29, H 5.91, N < 0.10; m.p. 167 °C (decomp.). FTIR: $\tilde{\nu}$ = 479 [vw, ν_{sym}(Me–Tl–Me)], 532 [s, ν_{asym}(Me–Tl–Me)]. FT-Raman: 479 vs. [ν_{sym}(Me–Tl–Me)], 538 [w, ν_{asym}(Me–Tl–Me)]. ^1H NMR ([D$_6$]DMSO): δ = 0.71 [d, $^2J_{Tl,H}$ = 423 Hz, 12 H, $Me_2TlO(2,6\text{-}iPr_2C_6H_3)$], 1.03 [d, $^3J_{H,H}$ = 6.9 Hz, 24 H, $Me_2TlO(2,6\text{-}iPr_2C_6H_3)$], 3.47 [sept, $^3J_{H,H}$ = 6.9 Hz, 4 H, $Me_2TlO(2,6\text{-}iPr_2C_6H_3)$], 6.12 [t, $^3J_{H,H}$ = 7.4 Hz, 2 H, $Me_2TlO(2,6\text{-}iPr_2C_6H_3)$], 6.68 [d, $^3J_{H,H}$ = 7.4 Hz, 4 H, $Me_2TlO(2,6\text{-}iPr_2C_6H_3)$] ppm. $^{13}C\{^1H\}$ NMR ([D$_6$]DMSO): δ = 23.0 [d, $^1J_{Tl,^{13}C}$ = 2922 Hz, $Me_2TlO(2,6\text{-}iPr_2C_6H_3)$], 24.5 [s, $Me_2TlO(2,6\text{-}iPr_2C_6H_3)$], 26.0 [s, $Me_2TlO(2,6\text{-}iPr_2C_6H_3)$], 111.5 [s, $Me_2TlO(2,6\text{-}iPr_2C_6H_3)$], 121.9 [s, $Me_2TlO(2,6\text{-}iPr_2C_6H_3)$], 137.1 [s, $Me_2TlO(2,6\text{-}iPr_2C_6H_3)$], 163.6 [s, $Me_2TlO(2,6\text{-}iPr_2C_6H_3)$] ppm.

$[Me_2TlO(2,6\text{-}Ph_2C_6H_3)]_2$ (7): 2,6-PhC_6H_3OH (0.246 g, 1.00 mmol) was added to a solution of $TlMe_3$ (0.250 g, 1.00 mmol) in diethyl ether (15 mL). The reaction mixture was stirred for 1 h and filtered. The resulting white powder was dissolved in THF (8 mL), and the solution was allowed to sit at 23 °C. After 1 d, the solution was filtered to yield **7** as colorless crystals (0.063 g, 0.13 mmol, 13%). $C_{40}H_{38}O_2Tl_2$ (959.44): calcd. C 50.06, H 3.99, N 0.00; found C 50.32, H 4.04, N < 0.10; m.p. 280 °C. FTIR: $\tilde{\nu}$ = 543 [w, ν_{asym}(Me–Tl–Me)]. FT-Raman: 479 [vs, ν_{sym}(Me–Tl–Me)]. ^1H NMR ([D$_6$]-DMSO): δ = 0.47 [d, $^2J_{Tl,H}$ = 421 Hz, 12 H, $Me_2TlO(2,6\text{-}Ph_2C_6H_3)$], 6.31 [t, 2 H, $Me_2TlO(2,6\text{-}Ph_2C_6H_3)$], 7.00 [d, $^3J_{H,H}$ = 7.4 Hz, 4 H, $Me_2TlO(2,6\text{-}Ph_2C_6H_3)$], 7.14 [t, $^3J_{H,H}$ = 7.4 Hz, 4 H, $Me_2TlO(2,6\text{-}Ph_2C_6H_3)$], 7.30 [m, 8 H, $Me_2TlO(2,6\text{-}Ph_2C_6H_3)$], 7.67 [d, $^3J_{H,H}$ = 6.9 Hz, 8 H, $Me_2TlO(2,6\text{-}Ph_2C_6H_3)$] ppm. $^{13}C\{^1H\}$ NMR ([D$_6$]DMSO): δ = 24.4 [d, $^1J_{Tl,C}$ = 2811 Hz, $Me_2TlO(2,6\text{-}Ph_2C_6H_3)$], 111.5, 125.5, 128.1, 129.6, 129.9, 131.5, 143.3, 165.5 [s, $Me_2TlO(2,6\text{-}Ph_2C_6H_3)$] ppm.

$Me_2TlO(2,4,6\text{-}tBu_3C_6H_2)$ (8): 2,4,6-$tBu_3C_6H_2OH$ (0.262 g, 1.00 mmol) was added to a solution of $TlMe_3$ (0.250 g, 1.00 mmol) in toluene (5 mL). The solution was stirred for 1 h. The light-yellow solution was filtered and concentrated to 1 mL. After sitting at –15 °C for 1 d, the reaction mixture was filtered to yield **8** as colorless rodlike crystals (0.100 g, 0.202 mmol, 20%). $C_{20}H_{35}OTl$ (495.85): calcd. C 48.44, H 7.11, N 0.00; found C 48.84, H 6.92, N 0.00; m.p. 176 °C. FTIR: $\tilde{\nu}$ = 546 [w, ν_{asym}(Me–Tl–Me)]. FT-Raman: 484 [vs, ν_{sym}(Me–Tl–Me)]. ^1H NMR ([D$_6$]DMSO): δ = 0.85 [d, $^2J_{Tl,H}$ = 431 Hz, 6 H, $Me_2TlO(2,4,6\text{-}tBuC_6H_2)$], 1.15 [s, 9 H, $Me_2TlO(2,4,6\text{-}tBuC_6H_2)$], 1.32 [s, 18 H, $Me_2TlO(2,4,6\text{-}tBuC_6H_2)$], 6.76 [s, 2 H, $Me_2TlO(2,4,6\text{-}tBuC_6H_2)$] ppm. $^{13}C\{^1H\}$ NMR ([D$_6$]-DMSO): δ = 26.6 [d, $^1J_{Tl,C}$ = 2882 Hz, $Me_2TlO(2,4,6\text{-}tBuC_6H_2)$], 31.3 [s, $Me_2TlO(2,4,6\text{-}tBuC_6H_2)$], 32.9 [s, $Me_2TlO(2,4,6\text{-}tBuC_6H_2)$], 34.0 [s, $Me_2TlO(2,4,6\text{-}tBuC_6H_2)$], 35.4 [s, $Me_2TlO(2,4,6\text{-}tBuC_6H_2)$],

Table 3. Crystallographic data for **4**–**8**.[a]

	4	**5**	**6**	**7**	**8**
Formula	$C_{16}H_{22}O_2Tl_2$	$C_{20}H_{30}O_2Tl_2$	$C_{28}H_{46}O_2Tl_2$	$C_{40}H_{32}O_2Tl_2$	$C_{20}H_{35}OTl$
F_r	655.08	711.18	823.39	959.44	495.85
Crystal system	monoclinic	triclinic	monoclinic	monoclinic	orthorhombic
Space group	$P2_1/n$	$P\bar{1}$	$P2_1/n$	$P2_1/n$	*Pnma*
a [Å]	9.697(4)	7.910(1)	9.999(2)	15.666(7)	10.989(1)
b [Å]	11.302(5)	16.143(2)	8.983(2)	14.349(6)	14.697(1)
c [Å]	16.456(7)	17.949(3)	16.357(3)	16.251(7)	12.618(1)
α [°]	90	107.003(2)	90	90	90
β [°]	96.594(6)	90.476(2)	101.768(2)	113.030(6)	90
γ [°]	90	102.913(2)	90	90	90
V [Å^3]	1792(1)	2129.8(5)	1438.3(4)	3362(3)	2037.9(3)
Z	4	4	2	4	4
F(000)	1184	1312	784	1824	976
$\rho_{calcd.}$ [g cm^{-3}]	2.429	2.218	1.901	1.896	1.616
μ [mm^{-1}]	17.965	15.122	11.210	9.608	7.927
T [K]	198(1)	198(1)	198(1)	173(1)	198(1)
R_1[b]	0.0838	0.0372	0.0190	0.0280	0.0222
wR_2[c]	0.2291	0.0901	0.0473	0.0660	0.0615

[a] In all cases, λ = 0.71073 Å. [b] $R_1 = [\Sigma||F_o| - |F_c||]/[\Sigma|F_o|]$ for $[F_o^2 > 2\sigma(F_o^2)]$. [c] $wR_2 = \{[\Sigma w(F_o^2 - F_c^2)^2]/[\Sigma w(F_o^4)]\}^{1/2}$.

120.0 [s, 2 H, $Me_2TlO(2,4,6\text{-}tBuC_6H_2)$], 127.0 [s, 2 H, $Me_2TlO(2,4,6\text{-}tBuC_6H_2)$], 135.2 [s, 2 H, $Me_2TlO(2,4,6\text{-}tBuC_6H_2)$], 166.8 [s, 2 H, $Me_2TlO(2,4,6\text{-}tBuC_6H_2)$] ppm.

Crystal Structure Determination: Crystals of **4**–**8** were isolated from the reaction mixtures as indicated above, or from dichloromethane (in the case of **5**) at 23 °C. Single crystals were coated with Paratone-N oil, mounted using a 20 micron cryo-loop, and frozen in the cold nitrogen stream of the goniometer. A hemisphere of data was collected with a Bruker AXS P4/SMART 1000 diffractometer using ω and θ scans with a scan width of 0.3° and 10 s exposure times. The detector distance was 5 cm. The crystal of **4** was a multiple twin and the orientation matrix for two major components was determined (CELL_NOW).[26] The crystal of **5** was a multiple twin and the orientation matrix for the major component was determined.[27] The structure of **5** contained two independent molecules in the asymmetric unit. The data were reduced (SAINT)[28] and corrected for absorption [TWINABS[29] (**4**), SADABS[30] (**5**–**8**)]. The structure was solved by direct methods and refined by full-matrix least-squares on F^2 (SHELXTL)[31] on all data. All non-hydrogen atoms were refined anisotropically. Hydrogen atoms were included in calculated positions and refined using a riding model. Crystallographic data are given in Table 3.

CCDC-740493 (for **4**), -767544 (for **5**), -740494 (for **6**), -740495 (for **7**), and -740712 (for **8**) contain the supplementary crystallographic data for this paper. These data can be obtained free of charge from The Cambridge Crystallographic Data Centre via www.ccdc.cam.ac.uk/data_request/cif.

Computational Methods: DFT calculations were performed using Gaussian 03[32] at the B3LYP 6-31G* level of theory for all atoms except Tl, for which Stuttgart electron-core pseudo-potentials (sdd) were employed. All structures were geometry-optimized, and structural parameters for input files were derived from crystal structure data where possible. Structural parameters for proposed monomeric structures were derived from the crystal structure data of **5**. Frequency calculations were performed on all structures and gave no imaginary frequencies. Energy values reported are the electronic energy values corrected for zero-point energies derived from frequency calculations.

Supporting Information (see footnote on the first page of this article): Complete FTIR and FT-Raman data for **4**–**8**, DFT-calculated bond lengths and angles for **4**–**8**, DFT-calculated surfaces (HOMO to HOMO–15) of $[Me_2TlO(2,6\text{-}Me_2C_6H_3)]_2$ (**5**), and X-ray crystallographic data for **4**–**8**.

[1] a) Z. Z. Zheng, A. M. Herrmann, *Nature* **1988**, *332*, 138–139; b) A. M. Herrmann, J. V. Yakhmi, *Thallium-Based High Temperature Superconductors*, Marcel Dekker Inc., New York, **1994**.

[2] a) R. J. Phillips, M. J. Shane, J. A. Switzer, *J. Mater. Res.* **1989**, *4*, 923–929.

[3] D. S. Richeson, L. M. Tonge, J. Zhao, H. O. Marcy, T. J. Marks, B. J. W. Wessels, C. R. Kannewurf, *Appl. Phys. Lett.* **1989**, *54*, 2154–2156.

[4] A. D. Berry, T. Holm, R. L. Mowery, N. H. Turner, M. Fatemi, *Chem. Mater.* **1991**, *3*, 72–77.

[5] G. Malandrino, A. M. Borzi, F. Castelli, I. L. Fragalà, W. Dastrù, R. Gobetto, P. Rossi, P. Dapporto, *Dalton Trans.* **2003**, 269–374.

[6] R. Amano, Y. Shiokawa, *Inorg. Chim. Acta* **1993**, *203*, 9–10.

[7] R. D. Pike, *Encyclopedia of Inorganic Chemistry* (Eds.: R. B. King), vol. 9, Wiley, Toronto, **2006**, and references cited therein.

[8] J. S. Casas, M. S. García-Esende, J. Sordo, *Coord. Chem. Rev.* **1999**, *193–195*, 283–359, and references cited therein.

[9] R. T. Griffin, K. Hendrick, R. W. Matthews, M. McPartin, *J. Chem. Soc., Dalton Trans.* **1980**, 1550–1555.

[10] Y. M. Chow, D. Britton, *Acta Crystallogr., Sect. B* **1975**, *31*, 1929–1934.

[11] a) R. C. Menzies, A. R. P. Walker, *J. Chem. Soc.* **1934**, 1131; b) G. E. Coates, R. A. Whitcombe, *J. Chem. Soc.* **1956**, 3351–3354.

[12] a) R. C. Menzies, *J. Chem. Soc.* **1930**, 1571–1573; b) A. G. Lee, G. M. Sheldrick, *J. Organomet. Chem.* **1969**, *17*, 481–484.

[13] A. G. Lee, G. M. Sheldrick, *Trans. Faraday Soc.* **1971**, *67*, 7–11.

[14] P. J. Burke, L. A. Gray, P. J. C. Hayward, R. W. Matthews, M. McPartlin, D. G. Gillies, *J. Organomet. Chem.* **1977**, *136*, C7–C10.

[15] H. Kurosawa, K. Yasuda, R. Okawara, *Bull. Chem. Soc. Jpn.* **1967**, *40*, 861–864.

[16] G. D. Shier, R. S. Drago, *J. Organomet. Chem.* **1966**, 330–340.

[17] For a study of corresponding indium analogues, see: G. G. Briand, A. Decken, N. S. Hamilton, *Dalton Trans.* **2010**, *39*, 3833–3841.

[18] a) H. Gilman, R. G. Jones, *J. Am. Chem. Soc.* **1946**, *68*, 517–520; b) R. Boese, A. J. Downs, T. M. Greene, A. W. Hall, C. A. Morrison, S. Parsons, *Organometallics* **2003**, *22*, 2450–2457.

[19] Individual $^2J(^1H–^{203}Tl)/^2J(^1H–^{205}Tl)$ and $^1J(^{13}C–^{203}Tl)/^1J(^{13}C–^{205}Tl)$ couplings could not be resolved due to peak broadening, although $^2J(^1H–^{203}Tl)$ values have been reported to be 2–4 Hz less than $^2J(^1H–^{205}Tl)$ in other dimethylthallium compounds (see ref.[15]).

[20] M. V. Castano, A. Sánchez, J. S. Casas, J. Sordo, J. L. Briansó, J. F. Piniella, X. Solans, G. Germain, T. Debaerdemaeker, J. Glaser, *Organometallics* **1988**, *7*, 1897–1904.

[21] P. J. Burke, L. A. Gray, P. J. C. Hayward, R. W. Matthews, M. McPartlin, *J. Organomet. Chem.* **1977**, *136*, C7–C10.

[22] G. Briand, A. Decken, N. S. Hamilton, *Dalton Trans.* **2010**, *39*, 3833–3841.

[23] A. V. Firth, J. C. Stewart, A. J. Hoskin, D. W. Stephan, *J. Organomet. Chem.* **1999**, *591*, 185–193.

[24] A. J. R. Son, M. G. Thorn, P. E. Fanwick, I. P. Rothwell, *Organometallics* **2003**, *22*, 2318–2324.

[25] H. Gilman, R. G. Jones, *J. Am. Chem. Soc.* **1946**, *68*, 517–20.

[26] G. Sheldrick, *CELL_NOW*, Bruker AXS, Inc., Madison, Wisconsin, USA, **2005**.

[27] For compound **5**, a power failure led to incomplete data collection (82% at 50° in 2θ). The sample decomposed at room temperature, and data collection could not commence after power was restored. The compound crystallizes as bundles of fibers, and the degree of fiber alignment results in multiple twins with one or more major components. Despite several attempts using various solvents and techniques (evaporation, cooling, and solvent diffusion), a second sample of a multiple twin with one major component or a single crystal could not be obtained. Complete data collection and structural refinement for several multiple twin crystals consistently yielded the same unit cell and structural solution. The results of both the original incomplete data set and a complete multiple twin data set have been submitted as Supporting Information

[28] *SAINT 7.23A*, Bruker AXS, Inc., Madison, Wisconsin, USA, **2006**.

[29] G. Sheldrick, *TWINABS 1.05*, Bruker Nonius, Inc., Madison, Wisconsin, USA, **2004**.

[30] G. Sheldrick, *SADABS*, Bruker AXS, Inc., Madison,Wisconsin, USA, **2004**.

[31] G. Sheldrick, *SHELXTL* 6.14, Bruker AXS, Inc., Madison, Wisconsin, USA, **2000**.

[32] M. J. Frisch, G. W. Trucks, H. B. Schlegel, G. E. Scuseria, M. A. Robb, J. R. Cheeseman, J. A. Montgomery Jr., T. Vreven, K. N. Kudin, J. R. Burant, J. M. Millam, S. S. Iyengar, J. Tomasi, V. Barone, B. Mennucci, M. Cossi, G. Scalmani, N. Rega, G. A. Petersson, H. Nakatsuji, M. Hada, M. Ehara, K. Toyota, R. Fukuda, J. Hasegawa, M. Ishida, T. Nakajima, Y. Honda, O. Kitao, H. Nakai, M. Klene, X. Li, J. E. Knox, H. P. Hratchian, J. B. Cross, C. Adamo, J. Jaramillo, R. Gomperts, R. E. Stratmann, O. Yazyev, A. J. Austin, R. Cammi, C. Pomelli, J. W. Ochterski, P. Y. Ayala, K. Morokuma, G. A. Voth, P. Salvador, J. J. Dannenberg, V. G. Zakrzewski, S. Dapprich, A. D. Daniels, M. C. Strain, O. Farkas, D. K. Malick, A. D. Rabuck, K. Raghavachari, J. B. Foresman, J. V. Ortiz, Q. Cui, A. G. Baboul, S. Clifford, J. Cioslowski, B. B. Stefanov, G. Liu, A. Liashenko, P. Piskorz, I. Komaromi, R. L. Martin, D. J. Fox, T. Keith, M. A. Al-Laham, C. Y. Peng, A. Nanayakkara, M. Challacombe, P. M. W. Gill, B. G. Johnson, W. Chen, M. W. Wong, C. Gonzalez, J. A. Pople, *Gaussian 03*, rev. D.01, Gaussian Inc., Wallingford, CT, **2004**.

Received: January 13, 2011
Published Online: March 30, 2011

